 doi:10.20944/preprints202207.0023.v1

Article

Nanostructured Electrospun Polycaprolactone - Propolis Films Composed of Different Morphologies for Potential Use in Wound Healing

Agnes C. de Figueiredo [1], Javier M. A. Mancipe [1,2], Aline O. da Silva de Barros [3,4], Ralph Santos-Oliveira [3,4], Marcos L. Dias [2] and Rossana M. S. M. Thiré [1*]

[1] Universidade Federal do Rio de Janeiro, COPPE/Program of Metallurgical and Materials Engineering - PEMM, 21941-599 Rio de Janeiro - RJ, Brazil
[2] Universidade Federal do Rio de Janeiro, Institute of Macromolecules Professora Eloisa Mano – IMA, 21941-598 Rio de Janeiro – RJ, Brazil
[3] Comissão Nacional de Energia Nuclear, Nuclear Engineering Institute - IEN, 21941-906 Rio de Janeiro - RJ, Brazil
[4] Universidade Estadual da Zona Oeste, Laboratory of Radiopharmacy and Nanoradiopharmaceuticals, 23070-200 Rio de Janeiro - RJ, Brazil
*Corresponding author: rossana@metalmat.ufrj.br; Phone: +55 21 3938-8500

Abstract: The structure of wound dressing materials presents one of the most relevant characteristics for effective skin tissue repair. Electrospinning is a common technique used to produce polymeric fibres that can mimic fibrillar disposition of skin extracellular matrix, favouring cell migration, and thus regeneration of the damaged tissue. Moreover, beads, also known as by-products of electrospinning, have potential as reservoirs for sustained drug release. Processing parameters, such as molecular weight and viscosity of the polymer solution, can affect the desirable morphologies of electrospun films. Thereby, this work had the purpose of producing and characterized electrospun polycaprolactone (PCL) mats loaded with propolis, a popular extract in traditional medicine with potential for skin repair aid. Films with different morphologies were obtained depending on the storage period of the solution prior to the lectrospinning, probably due to the PCL hydrolysis. FTIR analyses of the extract confirmed propolis composition. GPC and viscosity analyses demonstrated that the decrease in molar mass over the storage period was responsible for nanostructure diversity. Propolis acts as a lubricant agent, affecting the spun solutions' viscosity and the thermal properties and hydrophilicity of the films. All films are within the value range of the water vapour transpiration rate of the commercial products. The presence of beads did not affect the propolis release pattern. However, "in vitro" wound healing assay showed that propolis-loaded films composed by beaded fibres increased the cell migration process. Thus, it can be inferred that these films presented the potential for wound dressing application.

Keywords: electrospinning; morphology structures; propolis; polycaprolactone; drug delivery

1. Introduction:

One of the largest organs in the human body, the skin is essential to homeostasis. In addition of protecting against physical and chemical injuries, it also acts as a barrier against pathogens, controls water loss, is a sensory receptor, protects against ultraviolet radiation, converts precursor molecules into active vitamin D, contributes to body thermoregulation, and excretes substances [1]. For that reason, it is essential to recover the original tissue and its function when it is injured, avoiding function loss as in the scarring process [2].

Therefore, advances in regenerative medicine and the need for new alternative ways for wound healing promote the advent of new materials capable of miming skin extracellular matrix structures and their properties [3]. These biomaterials can be used for several

 doi:10.20944/preprints202207.0023.v1

critical skin wound regeneration, such as burns, injuries caused by trauma accidents, and even chronic wounds.

Among several methods for scaffold production, electrospinning is a technique capable of creating nanostructured films using polymer solutions. The system consists of an infusion pump, a high voltage source, a metallic collector, and a syringe with polymer solubilized in a conductive solvent. The films are effortlessly produced and able to replicate skin extracellular matrix structures [4-6]. Aside from acting as a barrier to pathogens while the tissue is repairing itself, they also provide a large surface area to volume ratio, which can be favourable for local drug delivery and have an ideal porosity for gas transition [7]. However, many variables must be evaluated for the desired morphology acquisition, including molar mass, polymer concentration, viscosity, surface tension, and conductivity of the polymer solution used. Furthermore, process variables, such as voltage and flow rate, and environmental factors, such as temperature and humidity, should be considered as well [8,9]. In literature, there is a focus on obtaining uniform fibres. However, some articles report that the presence of bead-like structures—considered as artefacts or by-products of fibres—make electrospun films more effective in drug loading and sustained release [10-12].

Among popular polymers used in the electrospinning method, there is polycaprolactone (PCL) due to its easy spinnability. PCL is a Food and Drug Administration (FDA) approved semi-crystalline polyester with potential for biomedical applications and delivery systems because of its biocompatible and biodegradable characteristics. It is one of the most used biopolymers for skin regeneration and is easy to process in various formats, producing films, membranes, or fibres [13,14].

Propolis (Prop) is a resinous bee mixture widely used in traditional medicine. Its composition varies according to the honeybees' food source and may contain more than 300 components [15]. Cheap and easy to find, its extract has antioxidant, anti-inflammatory, antimicrobial, and healing properties due to the presence of phenolic compounds and flavonoids in its composition [7,16-19]. In ideal concentration, propolis has the potential for skin repair aid and contributes to restraint pathogens. Oliveira et al [20], for example, developed a hydrophilic PVA/CMC dressing with propolis for burn treatment. More recently, Stojko [21] and Alberti [22] produced PLA and PVA electrospun fibres, respectively loaded with propolis, and Salimbeigi [23] produced nanofibres of PCL/propolis using chloroform/methanol (7:3) as system solvent also for wound healing applications.

PCL electrospinning has been commonly carried out using halogenated solvents such as 1,1,1,3,3,3-Hexafluoropropan-2-ol (HFIP), chloroform, and dichloromethane (DCM) as they have a good affinity for PCL, in addition to giving the solution a good electrical permittivity helping with spinning [24-26]. Such solvents, however, present high toxicity to the organism's cells, posing health risks. For this reason, the use of greener solvent systems such as acetic acid and formic acid for PCL solubilisation has been reported [27-35]. This mixture of solvents in several proportions was evaluated and its efficacy for PCL electrospun fibers production was proved. Moreover, it was reported that the acetic acid/formic acid system enables cost and toxicity reduction compared to more conventional solvents. While formic acid contributes to the solution's electrical permittivity, acetic acid is mainly responsible for polymer solubilisation [29]. This study aims to contribute to the advances in skin tissue engineering by producing and evaluating PCL/propolis electrospun films for potential use in wound healing. Different morphologies (fibres, beaded fibers, and beads) of PCL/Prop films were studied parallel to pure PCL samples. The physicochemical properties of the solutions and the electrospun films were analysed. Besides, the potential of the films for accelerating the wound healing was evaluated using an “in vitro” scratch wound healing model.

2. Results and Discussion:

2.1. Propolis Extract Chemical Composition Analysis by Fourier-Transform Infrared Spectroscopy (FTIR)

Preprints (www.preprints.org) | NOT PEER-REVIEWED | Posted: 1 July 2022 doi:10.20944/preprints202207.0023.v1

As the composition of propolis may vary depending on honeybees' food source, it is relevant to analyse its chemical composition, as there may be a presence or absence of some compounds.

Figure 1 shows the spectrum related to the propolis extract used in this study. Broad band at 3324 cm-1 is assigned to O-H group stretching vibrations, as well as to C-H, H-C of aromatics, O-H of flavonoid compounds, and N-H of amino acids [36]. Bands 2971 and 2919 cm-1 could be related to the asymmetric stretch of CH2 in ethanol, while 2840 cm-1 is assigned to its symmetric stretching. 1689, 1629, and 1600 cm-1 could be related to the stretching vibrations of C=C and C=O groups in flavonoids, and N-H asymmetric stretch vibrations of amino acids [37]. The band at 1511 cm-1 could be attributed to flavonoids and aromatic rings (deformations and stretching of C=C aromatic groups) [38]. 1373 cm-1 is cm-1 is associated with scissoring vibrations of C-H groups in hydrocarbons and flavonoids [39]. 1257 cm-1 could be assigned to C-O groups in polyols, such as hydroxy-flavonoids, or to wagging vibrations of C-H groups in phenolic compounds [31]. 1163 cm-1 is related to C-O stretching vibrations in lipids, and C-OH bending vibrations in tertiary alcohol groups [37,38]. 1080 cm-1 could be attributed to O-H of stilbenes, steroids, fatty acids, carboxylic acids, and secondary alcohols. This band is also assigned to C-O groups in flavonoids and terpenes [36]. The band 1039 cm-1 represents stretching vibrations of C-O ester groups and also primary and secondary alcohols [38]. 981 cm-1 is associated with scissoring vibrations of CH3 in esters [39].

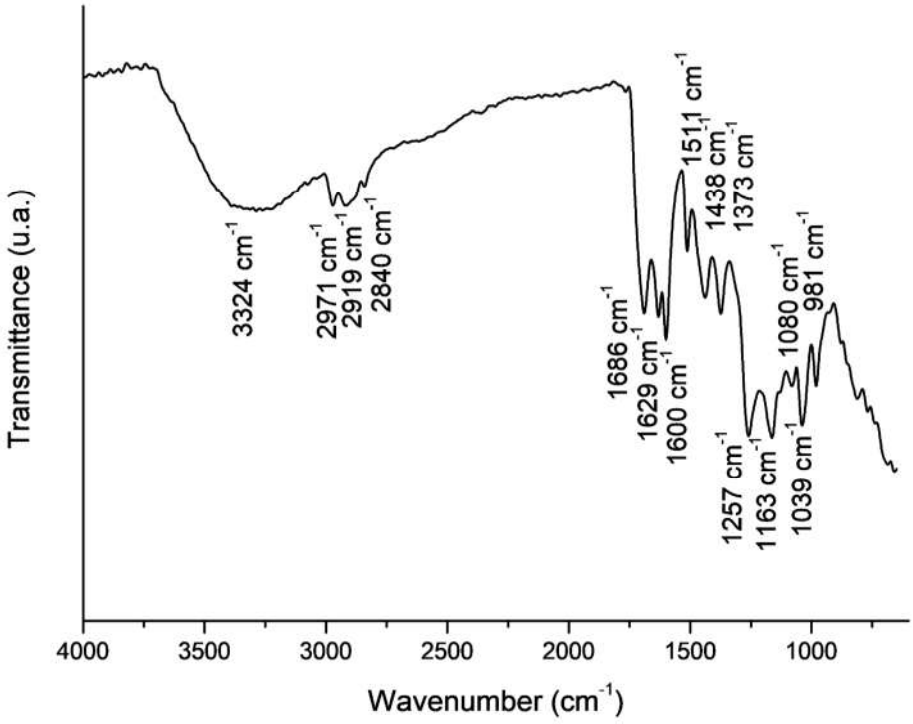

Figure 1. Fourier-Transform Infrared Spectroscopy bands related to the propolis extract..

2.2. Viscosity and Molecular Weight as Function of Solubilisation Time

Figure 2 shows viscosity, as well as polymer molar mass, which are two of the most important parameters in the electrospinning process as they describe the entanglement capacity of polymer chains that will result in fibre formation. Viscosity analysis was done on the solutions before processing, while number average molecular weight (Mn) analysis

Preprints (www.preprints.org) | NOT PEER-REVIEWED | Posted: 1 July 2022 doi:10.20944/preprints202207.0023.v1

was performed on electrospun films (using solutions with 1, 7, and 14 days of storage time).

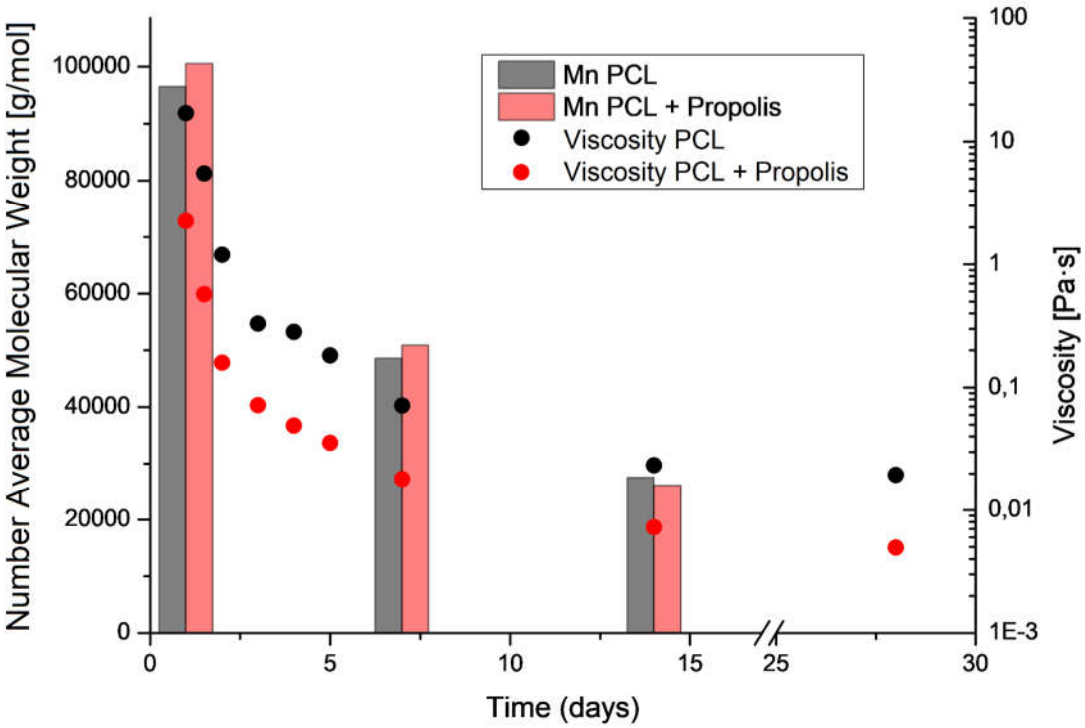

Figure 2. Number average molecular weight and viscosity for PCL and PCL + Propolis solutions after days of dissolution.

The viscosity values of both solutions have decreased over time, as an exponential-like behaviour attributed to PCL hydrolysis due to exposure to the AA/AF solvent system. At all times tested, up to 28 days, the PCL + Propolis solution was always less viscous than the pure PCL one, which agrees with the behaviour observed for propolis/PVP solution viscosity evaluated by Moghaddam [40]. On the other hand, gel permeation chromatography analysis of electrospun films on days 1, 7, and 14 indicates that Mn values for PCL in PCL solution and in PCL + Propolis solution had an approximately 50% decrease each week spent in storage. These results corroborate the viscosity values, although they imply that the propolis extract addition does not affect the polymer Mn but acts as a lubricating agent, which increases the free volume and the mobility of polymer chains [41].

According to Dias et al. [42], the viscosity of the solution is related to the entanglement of polymer chains. The reduction of these entanglements, whether due to low polymer concentration or low molecular weight, affects the spinning process as a result of the Taylor cone's destabilisation, which can generate defective fibres or even only bead films [8,27]. Nevertheless, Lavielle et al. [30] and Gil-Castell et al. [32], although evaluating PCL in different concentrations and using an AA/FA solvent system in a different ratio, reported similar decreases in molecular weight within eleven and five days, respectively. It was suggested that when using the mixture as a solvent, PCL is subjected to degradation by acid hydrolysis [30], which generates instability in electrospinning.

Preprints (www.preprints.org) | NOT PEER-REVIEWED | Posted: 1 July 2022 doi:10.20944/preprints202207.0023.v1

2.3. Morphology and Fibre Diameter in the Electrospun Films

A decrease in Mn was evidenced according to the results previously observed. As discussed, Mn is a variable related to the viscosity of the polymer solution (Figure 2), directly influencing the morphology of the electrospun fibres. Solutions of PCL and PCL with propolis extract were electrospun by varying the flow rate and applied voltage. The films obtained were evaluated by scanning electron microscopy (SEM) (Figure 3), and Table 2 presents the best conditions for morphology acquisition, generating a total of 6 samples, PCL and PCL + Propolis films. The diameter of the structures was quantified by an image treatment carried out with SizeMeter 1.1 software (Table 3).

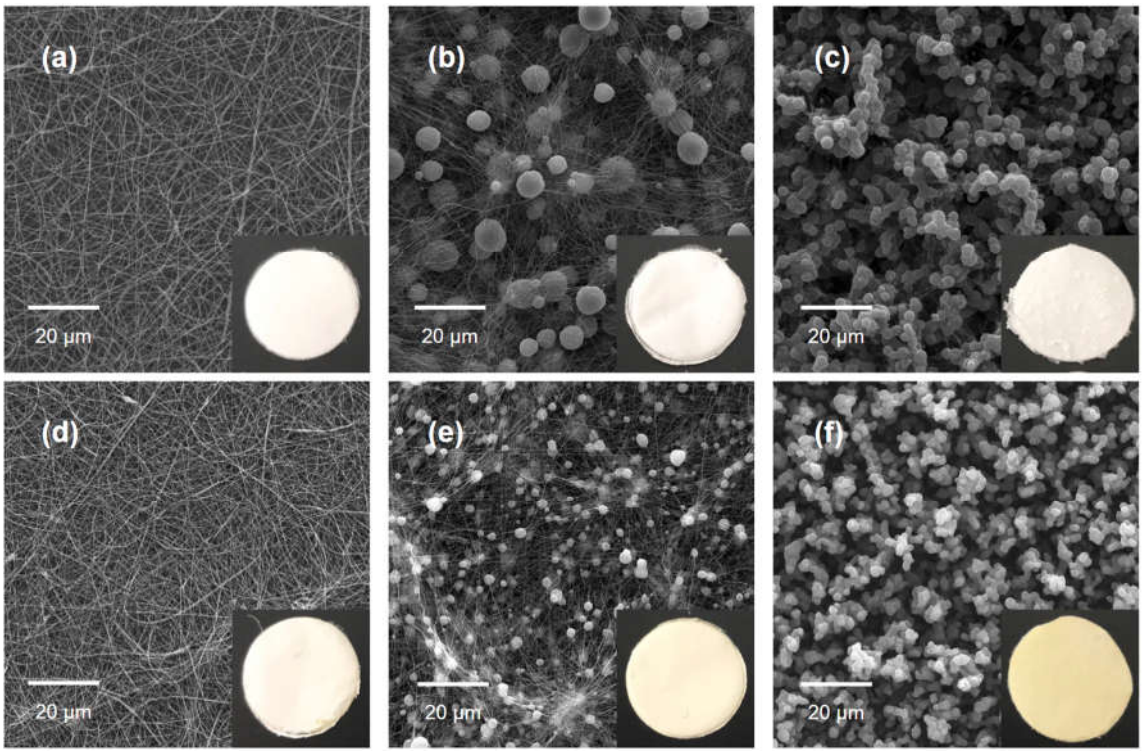

Figure 3. Scanning electron microscopy images and macrography (disks of 1.5 cm diameter) of electrospun films. (**A**) PCL fibres; (**B**) PCL beaded fibres; (**C**) PCL beads; (**D**) PCL/Prop fibres; (**E**) PCL/Prop beaded fibres; (**F**) PCL/Prop beads.

Table 2. Optimal values for sample production.

Variable	Fibres	Beaded Fibres	Beads	
PCL Concentration	30	30	30	% (w/v)
Distance needle tip/collector	10	10	10	cm
Flow Rate	2.0	1.0	1.0	mL/h
Voltage	10	15	15	kV
Storage at 35 ºC	1	7	14	days

 doi:10.20944/preprints202207.0023.v1

Table 3. Fibre and bead diameter measured in SizeMeter 1.1 software.

Sample	Diameter (nm)	
	Fibre (nm)	Bead (nm)
PCL Fibres	291.1 ± 59.4	-
PCL Beaded Fibres	137 ± 51.6	6,187.9 ± 1,885
PCL Beads	-	2,840.6 ± 557.1
PCL/Prop Fibres	201.1 ± 53.5	-
PCL/Prop Beaded Fibres	144.1 ± 44.2	2,545.8 ± 655.5
PCL/Prop Beads	-	1,255.4 ± 499.4

As observed in Figure 3, it was observed that PCL and PCL/Propolis solutions were immediately electrospun after solubilisation generated uniform and continuous fibres, while 7-day storage resulted in a decrease in the average fibre diameter and the occurrence of beads**.** On the other hand, the increase of the storage time to 14 days generated only beads film, morphology also previously reported [43, 44].

The differences among morphologies could be explained by the solution's exposure time to the solvent system as it changes the polymer molecular weight and viscosity. As reported by Haider et al. [4], a decrease in molecular weight, and consequently in viscosity, turn the Taylor Cone less stable as the polymer chains are less entangled and susceptible to breaking due to the voltage and surface tension before reaching the collector, which will entail gross defects in film morphology (appearance of beads and higher standard deviation of fibre diameters). At 14 days of exposure, due to the significant decrease in PCL molecular weight, the electrospinning process is differentiated and usually referred to as electrospray [45].

Once defects in fibres are present, there is also a drastic decrease in fibre diameter (compared to only fibres samples), as seen in Figure 3b and Figure 3e. This is related to the use of low concentration and/or low molar mass polymer solutions. In both cases, it relates the density of chain entanglements to the stability of the Taylor cone [29,46].

Moreover, the films' macrographs also allow observing an increase of colour in PCL/Prop samples as the solution storage time increases, especially in beads film. The yellowness is characteristic of the natural extract, which acts as a lubricant agent, as suggested in viscosity analysis.

2.4. Thermal Analysis by Differential Scanning Calorimetry (DSC)

Figure 4 shows the thermal transitions of PCL and PCL/Propolis electrospun samples as well as the thermal behaviour of electrospun films from solutions stored at 1, 7, and 14 days evaluated by differential scanning calorimetry (DSC). The melting temperatures (T_m), enthalpies (ΔH_m), and degree of crystallinity (Xc) for each thermal transition in the first and second heat cycles are displayed in Table 4.

 doi:10.20944/preprints202207.0023.v1

Table 4. Thermal transitions refer to the heating and cooling cycles of PCL and PCL + Propolis for the different morphologies.

Samples		First Heat Cycle			Second Heat Cycle		
		T_m (°C)	ΔH_m (J/mg)	Xc (%)	T_m (°C)2	ΔH_m (J/mg)2	Xc (%)
PCL	Fibres	68.4	26.4	17.4	57.0	27.1	17.9
	Beaded Fibres	71.1	51.2	33.8	62.0	38.3	25.2
	Beads	65.7	65.8	43.4	61.4	54.9	36.2
PCL + Prop	Fibres	71.4	31.3	20.6	64.3	28.0	18.5
	Beaded Fibres	67.3	54.4	35.9	62.0	42.0	28.0
	Beads	64.5	65.5	43.2	58.0	54.0	36.0

Preprints (www.preprints.org) | NOT PEER-REVIEWED | Posted: 1 July 2022 doi:10.20944/preprints202207.0023.v1

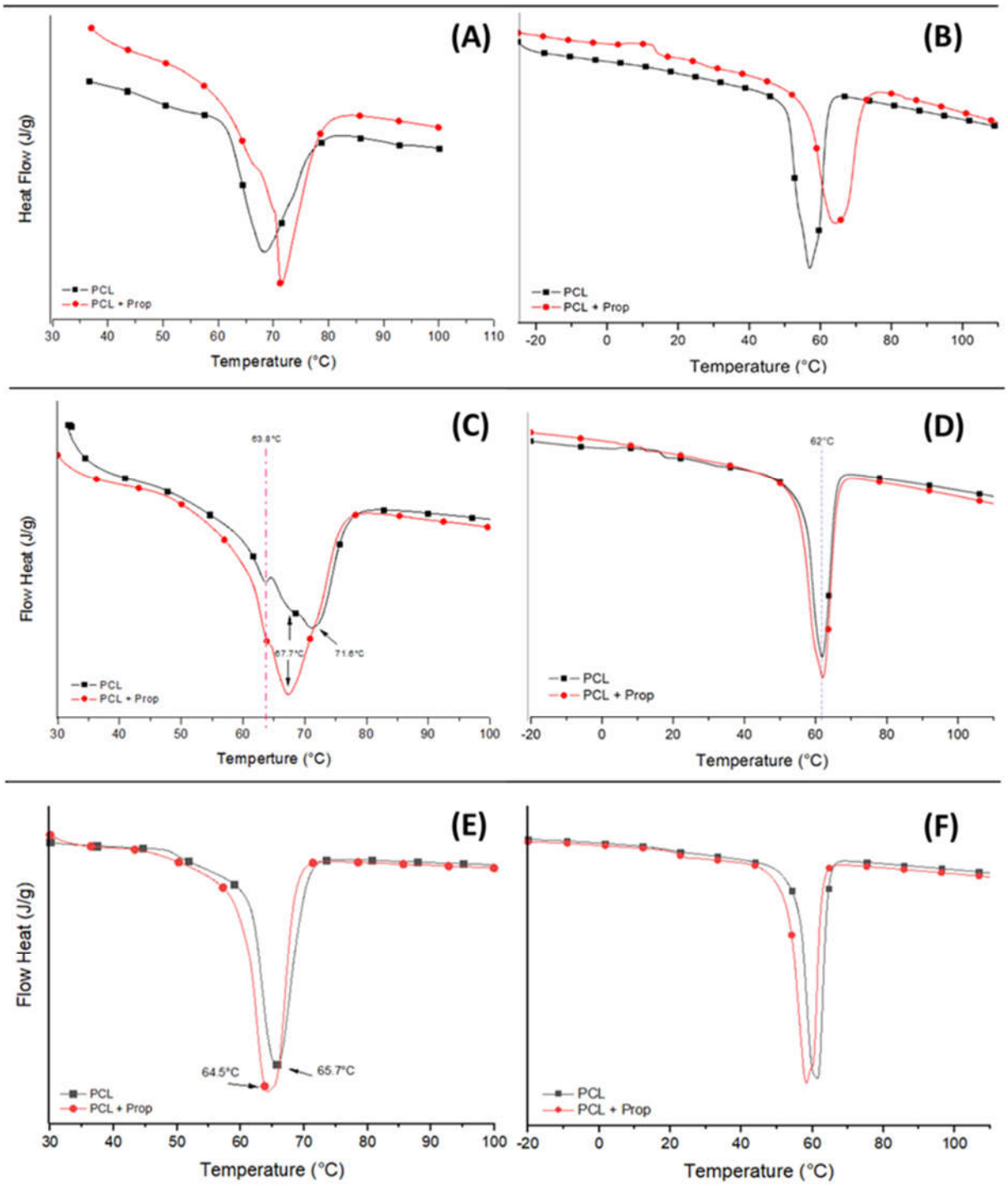

Figure 4. Differential scanning calorimetric thermograms for electrospun PCL and PCL + Propolis mats: first and second heating, respectively. (**A**, **B**) Fibres, (**C**, **D**) Beaded fibres, and (**E**, **F**) Beads.

In Figure 4a, fibres with propolis incorporation presented two endothermic peaks. The one allocated at 71 °C is attributed to the melting of a population of more perfect crystals compared to the crystal population on pure PCL fibres melted at the same point. On the other hand, the second peak close to 64 °C is attributed to another population of crystals not seen on the pure PCL fibre thermogram. Therefore, this peak can be assigned to PCL and propolis interactions, which favoured the formation of this more imperfect type of crystals [47].

Preprints (www.preprints.org) | NOT PEER-REVIEWED | Posted: 1 July 2022 doi:10.20944/preprints202207.0023.v1

For the electrospun samples exposed to 7 days of storage (beaded fibre morphology), the presence of two endothermic peaks was also observed, showing the presence of two populations of crystals as well (Figure 4c). However, the population melting at approximately 64 °C showed a higher intensity compared to the crystals of PCL/Prop fibres, demonstrating a formation of more crystals that may be granted to the packaging of smaller chains due to hydrolysis of the PCL in acetic acid.

Finally, the thermal transitions of the electrospun beaded structures (Figure 4e) demonstrated a greater bundling of the chains attributed to a lower molecular weight as seen in the GPC analysis (Figure 2), which generates an only population of crystals for both pure PCL and PCL/Prop at 65 °C approximately. Comparing the first and the second heatings of both types of beads and taking into account their Xc, there seems to have been no interactions between the lower molecular weight PCL and the propolis [48,49], which could also explain why PCL/Prop beaded film presents such intense yellow colour and corroborate with the interpretation of viscosity analysis.

2.5. Wettability Analysis

The wettability of the samples was evaluated through water contact angle (WCA) measures as shown in Figure 5. In this analysis, one water drop is allocated on every film with and without propolis extract with morphology variation.

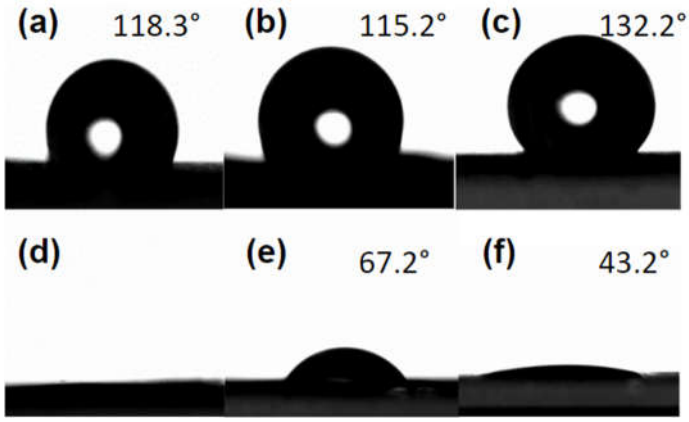

Figure 5. Water contact angle for electrospun samples with morphological variation. (**A**) PCL fibres; (**B**) PCL beaded fibres; (**C**) PCL beads; (**D**) PCL/Prop fibres; (**E**) PCL/Prop beaded fibres; (**F**) PCL/Prop beads.

Even though PCL films presented slight variations in the contact angle attributed to the surface roughness related to the specific morphology of each film, they still confirm PCL hydrophobic nature [50]. Although PCL has good biocompatibility, this poor wettability due to low surface energy can hinder cell adhesion [51]. Thus, when designing PCL based dressing, this should be a major consideration since PCL is a hydrophobic polymer [13].

On the other hand, the addition of propolis extract to the mats results in a significant decrease in contact angle measurements, which indicates an increase in the wettability of the films. The fibre mats WCA couldn't even be measured as the water drop deposited was immediately absorbed. This more hydrophilic nature can be attributed to the composition of propolis extract that, although it varies according to its origin, it has a high prevalence of terpenoids, phenolic acids, and flavonoids [52,53]. These compounds have a polar character due to their oxygenated groups, which favours the interaction with water and reduces the average contact angle on the samples. These results are in accordance with the studies of Li [54], where the authors evaluated different coatings of polydopamine (rich in polar groups) in PCL electrospun films, generating changes in PCL samples, from hydrophobic to super hydrophilic.

Preprints (www.preprints.org) | NOT PEER-REVIEWED | Posted: 1 July 2022 doi:10.20944/preprints202207.0023.v1

The WCA for the PCL/Prop beaded fibres mat is larger than the measurement for the PCL/Prop beads film, which can be explained by the diameter of the structures found in both samples. In addition to fibres, the beaded fibres film has beads approximately twice the size of the structures in beads film. This result is in agreement with Jia [55]: larger structures form more prominent cavities and trap more air between the water drop and the film surface, which results in a more hydrophobic state.

2.6. Water Vapour Transpiration Rate (WVTR) Analysis

The water vapour transpiration rate (WVTR) analysis evaluates the moisture conditions that a potential dressing can provide for a wound. In this study, WVTR analysis were carried out in electrospun samples with and without propolis, evaluating the water vapour cross the films as represented in Figure 6. From these values we calculated the WVTR shown in Table 5.

In this study, we used the second stage as a reference to the diffusion process in the films, described by Fick's law, and calculated the mass variation over time [56]. Later calculations were also made to find their transpiration flow. The rates of electrospun films ranged from 1263.08 to 2179.84 $g.m^{-2}$ per day, values within the range of WVTR of commercial dressings characterised mainly by large porosity, such as foams [57]. Thus, all samples achieved permeability values within the effective wound treatment range reported in the literature, as the rates on healthy skin are 204 g/m^2 per day and on wounded skin, 279-5138 $g.m^{-2}$ per day [58], and possibly could prevent exudate accumulation as well as excessive dehydration.

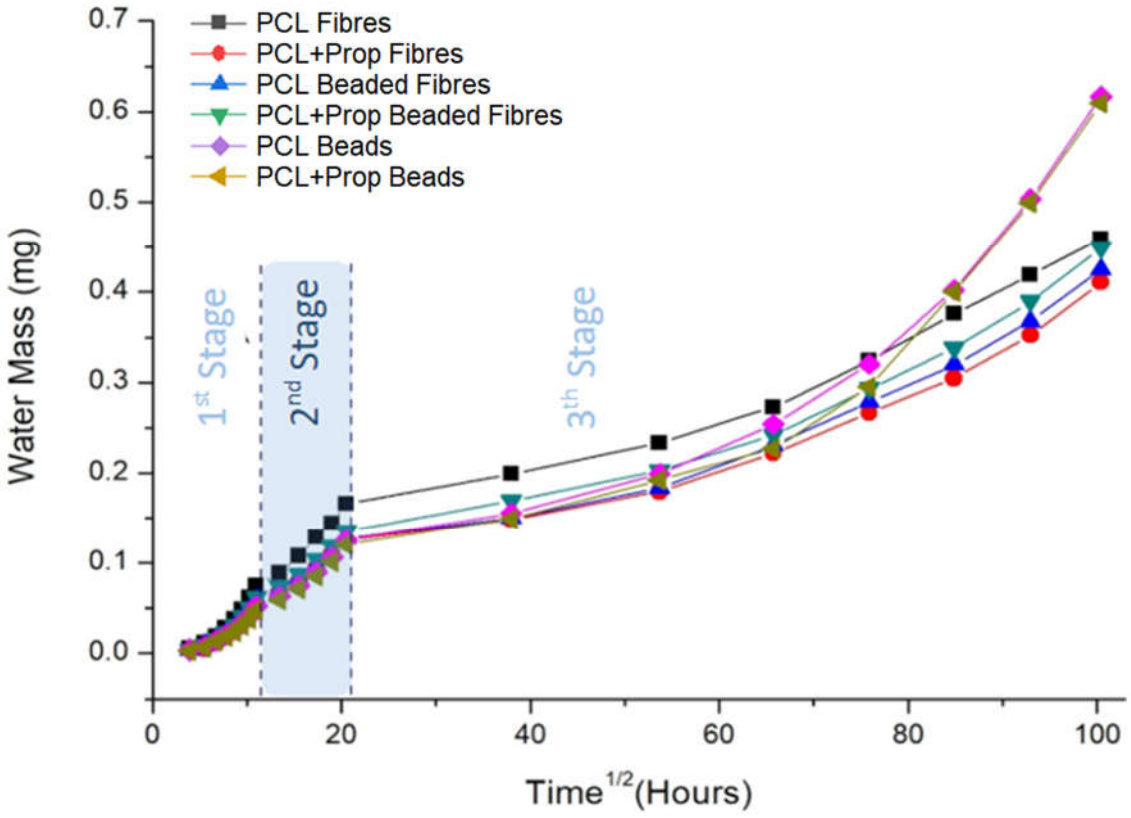

Figure 6. Water vapour flow (J) in electrospun films with morphology variation.

Preprints (www.preprints.org) | NOT PEER-REVIEWED | Posted: 1 July 2022 doi:10.20944/preprints202207.0023.v1

Table 5. Water vapour transpiration rate calculated by every sample with morphological variation from the water vapour flow (*J*).

Samples		*J*= Δm/Δt [mg/min]	Thickness [mm]	Water vapor transpiration rate [g/m² per day]
PCL	Fibres	0.0107	0.09	2179.84
	Beaded Fibres	0.0081	0.56	1650.16
	Beads	0.0088	0.48	1792.77
PCL/Prop	Fibres	0.0082	0.24	1670.53
	Beaded Fibres	0.0087	0.39	1772.39
	Beads	0.0086	0.14	1263.08

2.7. Propolis Release Analysis

To evaluate the delivery of the propolis encapsulated in the electrospun PCL structures, a release assay was performed for different times up to 48 hours, as shown in Figure 7. This was quantified using a UV-Vis spectrometer. PCL/Propolis samples were evaluated for 48 hours at 37° C and 100 rpm in a Shaker incubator.

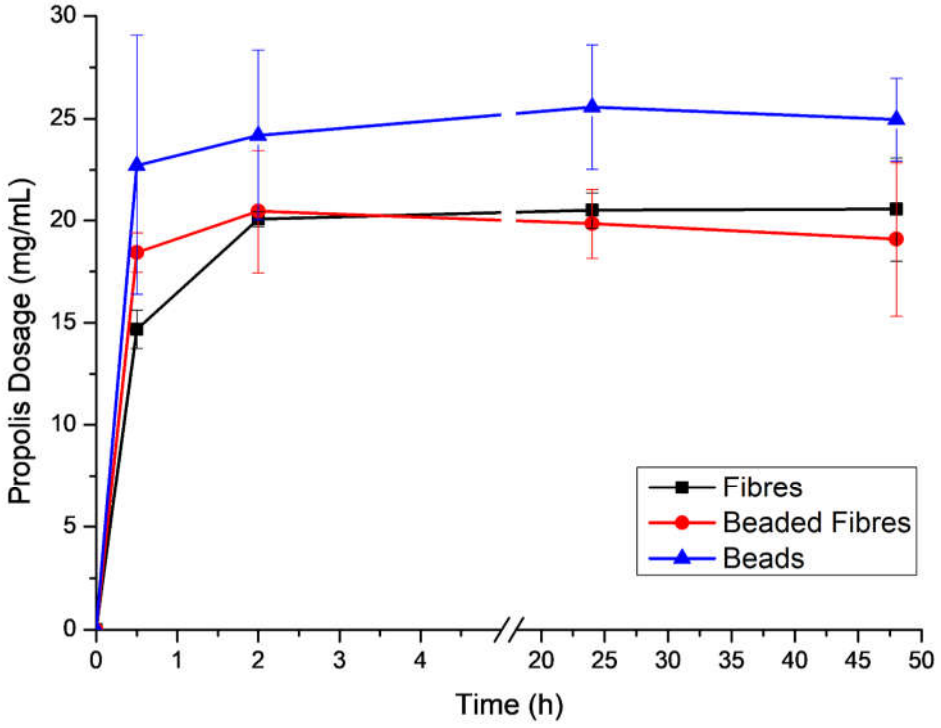

Figure 7. Propolis release profile in the function of the delivery time for the different morphologies.

Electrospun films have good properties for potential biological applications, such as a large surface area to volume ratio and high porosity that facilitates permeation. Those characteristics, however, also facilitate diffusion. Therefore, a similar burst release tendency was observed in all films in the first 30 minutes of the trial, even though several

Preprints (www.preprints.org) | NOT PEER-REVIEWED | Posted: 1 July 2022 doi:10.20944/preprints202207.0023.v1

works reported that the presence of beads in the electrospun structures could result in more sustained delivery time due to the increase in diameter film and/or layers in which said active components would have to diffuse through for release [10-12]. However, it seems that PCL/Prop fibres only reached their equilibrium concentration release after 2 h, which was equal to those of beaded fibres. Films composed only by beads presented a higher maximum concentration released of propolis.

Furthermore, at 37 ºC PCL is above the glass transition temperature, which increases polymer chain mobility [59]. As propolis is more hydrophilic and has more affinity with the aqueous medium than with the polymer matrix and acts as a lubricating agent, enlarging the PCL free volume, the extract diffusion is favoured. These features promote the burst effect *in vitro*, as also shown by Ramalingam et al. [60] and Maver et al. [61].

Besides that, the PCL/Prop beads morphology sample showed a slight increase in the releasing of propolis that could also be related to the porosity of the film. These films also immobilized a slightly higher amount of propolis than those containing fibres (fibres and beaded fibres). Although there is no evidence of good interaction between extract and polymer as seen previously, larger pores of the beads film could allow better penetration and contact with saline through the structure, which may have favoured the diffusion process.

Furthermore, some works described that drug delivery from nanostructured mats could also be influenced by other mechanisms besides diffusion, such as swelling [62]. Likewise, probably this is present in the PCL mats release pattern, as analysed by SEM after the release test (Figure 8). Samples' diameters were compared before and after the release test. This data is presented in Table 6.

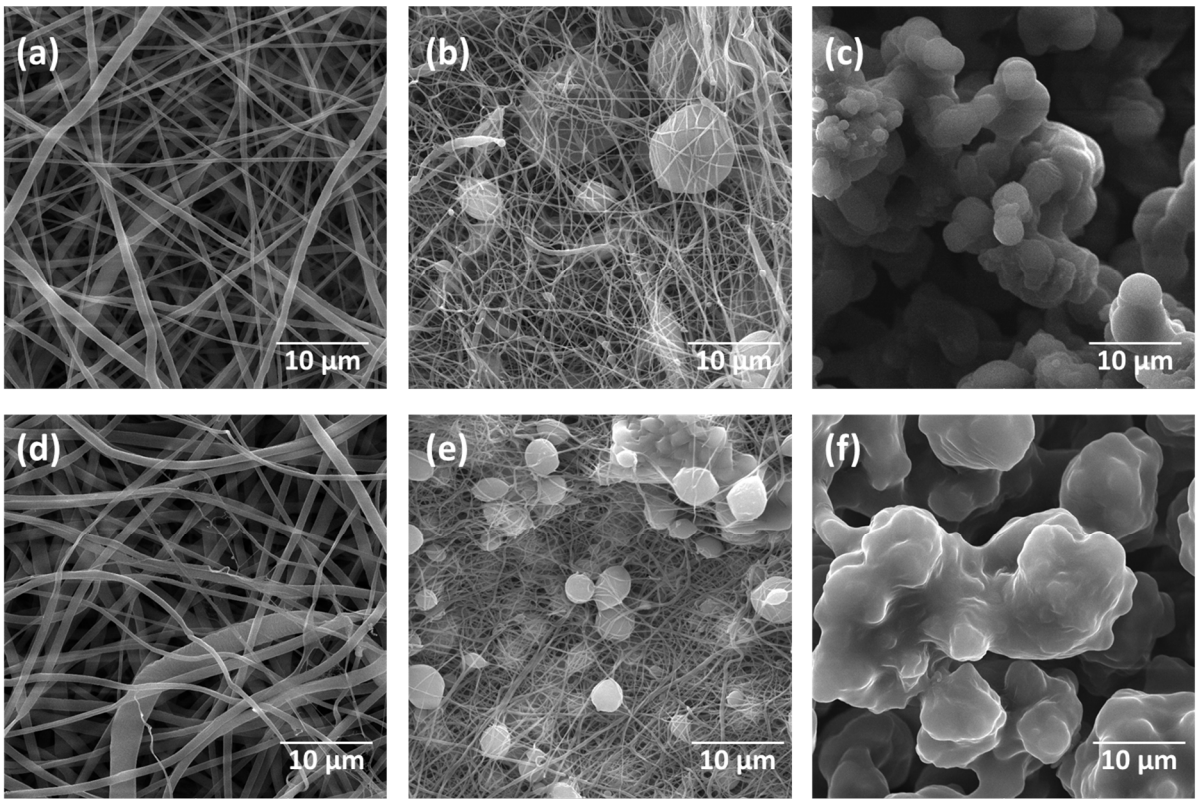

Figure 8. Scanning electron microscopy imagens of membranes with different morphologies after swelling and propolis release (48 h). PCL (**A**, **B**, **C**) and PCL + Propolis (**D**, **E**, **F**).

Preprints (www.preprints.org) | NOT PEER-REVIEWED | Posted: 1 July 2022 doi:10.20944/preprints202207.0023.v1

Table 6. Diameters before and after swelling and propolis release. Fibre and bead diameter after release assay measured in SizeMeter 1.1 software.

Samples	Diameter (nm)			
	Fiber		Bead	
	Before	After	Before	After
PCL Fibers	291.1 ± 59.4	811.1 ± 381.0	-	-
PCL Beaded Fibers	137 ± 51.6	461.2 ± 220.9	6,187.9 ± 1,885	6,199.6 ± 3,280.9
PCL Beads	-	-	2,840.6 ± 557.1	4,210.6 ± 1,177.9
PCL+Prop Fibers	201.1 ± 53.5	1,098.5 ± 478.3	-	-
PCL+Prop Beaded Fibers	144.1 ± 44.2	349.8 ± 109.9	2,545.8 ± 655.5	2,889.6 ± 910.6
PCL+Prop Beads	-	-	1,255.4 ± 499.4	-

Both PCL and PCL/Prop fibre films showed an increase in the diameter of their structures after immersion in saline solution for release testing, indicating a swelling pattern. Similar results were obtained in the studies of Reshmi et al. [63], in which PCL and PCL + nano chitosan fibres become swollen after 28 days in phosphate-buffered saline solution (PBS).

On the other hand, the fibres diameter of beaded fibre films also increased, but on a smaller scale compared to only fibre films. Their beads, however, did not seem to have had a significant increase of diameter, which leads to the understanding that diffusion may have contributed more to the release of propolis in this film structure than the swelling mechanism.

Additionally, the bead-only films demonstrated a visible swelling pattern only on the pure PCL films. In the case of PCL/Prop films, the structures were not measurable, as they appear to have melted, which suggests that the release of the extract—as it acts as a lubricating agent in a lower molecular weight sample— may have abruptly altered its morphology.

2.8.". In vitro" Wound Healing Assay

The scratch wound assay was used to investigate cell migration in the presence of the samples after a gap in a confluent monolayer of cells had been created to mimic a wound. Since cell migration is a crucial step for wound healing, this test can be used to estimate the "in vitro" capacity of the films to accelerate the healing. The results are shown in Figure 9 and Figure 10.

Preprints (www.preprints.org) | NOT PEER-REVIEWED | Posted: 1 July 2022 doi:10.20944/preprints202207.0023.v1

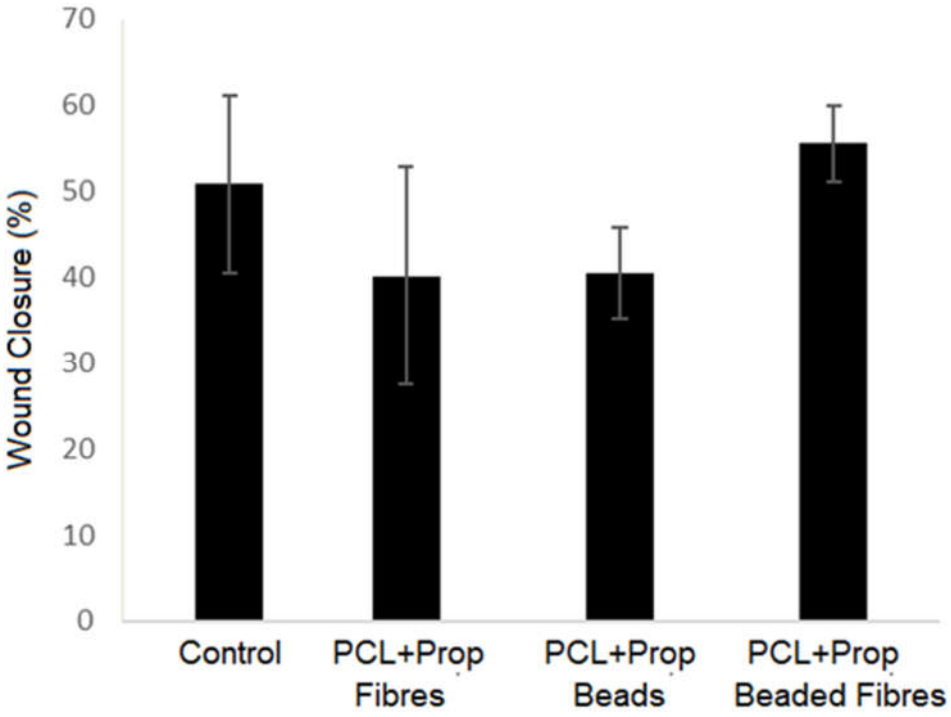

Figure 9. Quantitative analysis of fibroblasts migration area after 24 hours of wound healing in the presence of PCL/Prop films. Cells cultivated without any film were used as control.

PCL/Prop beaded fibre film had the most prominent results, since it could increase the healing in 24 hours by fastened the migration cell to the gap (Figure 9 and Figure 10). On the other hand, the presence of propolis in fibres films and in beaded films showed no significant effect in wound healing rate as compared to the control.

The wound-healing effect of propolis loaded in has been demonstrated by several "in vitro" and "in vivo" studies using different nanosystems for propolis delivery [64-71]. For example, Alberti et al [72] observed a wound site reduction of 68% after 7 days of *in vivo* and *in vitro* treatment using nanofibres of polyvinyl alcohol (PVA) and propolis. However, to our knowledge, no study was conducted before with PCL/propolis electrospun films. Besides, it is important to highlight that the healing capacity of this extract depends on the concentration and the type of propolis used.

Preprints (www.preprints.org) | NOT PEER-REVIEWED | Posted: 1 July 2022 doi:10.20944/preprints202207.0023.v1

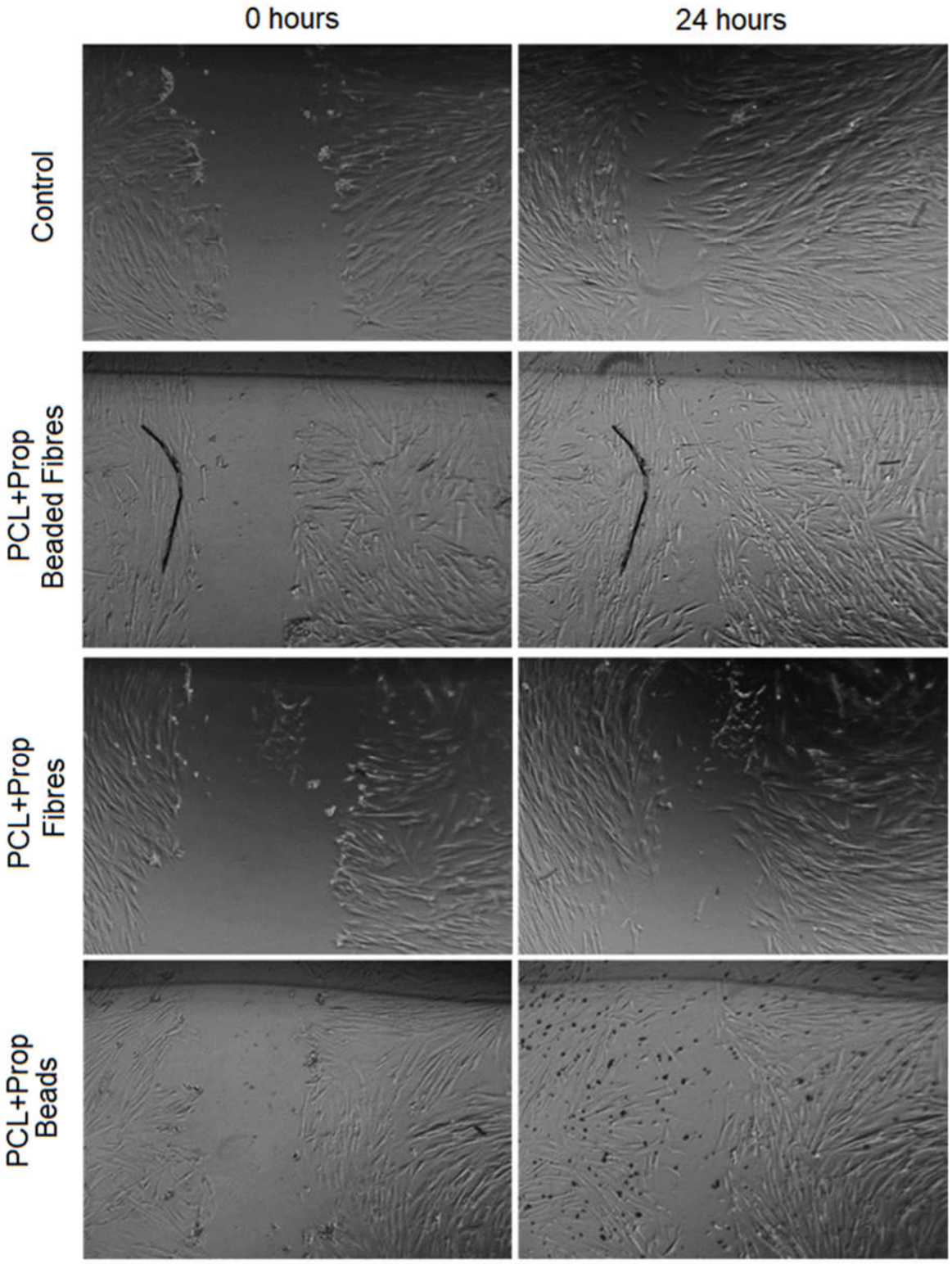

Figure 10. Evaluation of the scratch wound healing assay using human gingival fibroblast (FGH) cell staining with microscopic inspection of cells stained immediately after scratching (0 h) and after 24 h of wound healing.

In this study, the presence of propolis in a mixed nanostructured form increased the migration process. Since the propolis release pattern of the films were very similar, considering the propolis extract used, the positive response to FGH cells could be more related to the morphology, in particular surface roughness and wettability, than to the

Preprints (www.preprints.org) | NOT PEER-REVIEWED | Posted: 1 July 2022 doi:10.20944/preprints202207.0023.v1

presence of propolis. However, further studies should be conducted to evaluate the effect of the propolis concentration on the cell response to the PCL/propolis beaded fibre films.

3. Materials and Methods:

Film samples were produced using PCL pellets by Sigma-Aldrich Brazil (Mn: 80,000 g/mol, degree of hydrolysis of 98 mol %) purchased from Sigma-Aldrich, São Paulo, SP, Brazil, while glacial acetic acid (AA) and 98% pure formic acid (FA) were purchased from Vetec Química Fina LTDA. Alcoholic extract of Brazilian green propolis (minimum of dry extract of 11% w/v) was purchased from Apis Flora Indústria Brasileira, São Paulo, Brazil.

3.1. Fourier-Transform Infrared Spectroscopy (FTIR) Analysis

The Fourier-Transform Infrared Spectroscopy (FTIR) analysis with attenuated total reflectance (ATR) accessory to evaluate the chemical composition of the propolis extract was performed on a stored overnight (35 ºC) dry sample. The equipment used was Perkin Elmer Spectrum 100, 64 scans in the region of (4000-650) cm-1.

3.2. Polymeric Solutions

Two 30% m/v of PCL solutions were prepared using acetic acid and formic acid (9:1) as solvent systems according to Mancipe et al [27]. 15% v/v of propolis extract was added to the second solution [72]. Both were solubilized at room temperature for 12 hours with constant mechanical stirring. Subsequently, the solutions were immediately subjected to electrospinning or stored at 35 °C for up to 28 days to evaluate the polymer exposure to the solvent mixture.

Spinning conditions (Table 7) focused mainly on the flow rate, voltage, and solution storage time to obtain optimal values for production of PCL films and PCL-propolis extract films with three different morphologies (fibres, beaded fibres, and beads). Then, once established the electrospinning conditions, the solutions were electrospun for 2 hours to get films with adequate thickness for easy manipulation and subsequent characterisation.

Table 7. Main electrospinning variables evaluated.

Variable	Value	
PCL Concentration	30	% (w/v)
Distance needle tip/collector	10	cm
Flow Rate	1.0 - 2.0	mL/h
Voltage	10 - 15	kV
Molar Mass	26,500 - 100,517	g/mol
Humidity	50-70	%

3.3. Viscosimetry and Gel Permeation Chromatography (GPC) Analysis

Viscosity analysis of the polymeric solutions was performed with a rotational test on the Physica MCR 501 Anton Paar rheometer, with cone plate geometry; gap: 0.1 mm; 0 - 150 [1/s] and measured at 1 [1/s]. The solution viscosity was subjected to daily analysis for up to 7 days and then at 14 and 28 days of storage time. Average number molecular weight was evaluated using electrospun films obtained from solutions stored for 1, 7, and 14 days by Shimadzu LCSolution gel permeation chromatography (GPC) equipment to corroborate the viscosity analysis. Approximately 4 mg of electrospun samples were analysed using chloroform as solvent and injection volume of 2 μL. For the molecular weight determination, a calibration curve based on monodisperse polystyrene was used.

 doi:10.20944/preprints202207.0023.v1

3.4. Scanning Electron Microscopy (SEM)

Film samples were golden coated and evaluated using VEGA3 TESCAN (Czech Republic) scanning electron microscopy with 15 kV acceleration for morphology evaluation. Fibre and bead diameters were obtained using Size Meter 1.1 software (50 measurements for each film).

3.5. Thermal Characterisation

Differential scanning calorimetry (DSC) was carried through in a Hitachi – DSC 7020 Thermal Analysis system to study the thermal behaviour of the electrospun films. 7.0 mg of each sample was subjected to two heating cycles and one cooling cycle carried out at a rate of 10 ºC/min using nitrogen atmosphere with a flow rate of 50 mL/min. The first heating cycle was conducted from 25 to 90 ºC, followed by a cooling cycle to 0ºC and subsequent heating from 0 to 90 ºC. The degree of crystallinity of the material (Xc) was calculated by Equation 1.

$$X_c = \frac{\Delta H_f}{\Delta H_f^o} \quad (1)$$

Where ΔHf corresponds to the melting enthalpy of the endothermic peak of the DSC thermogram (second heating), while ΔH°_f = 151.7 J/g, is the theoretical melting enthalpy for a 100% crystalline PCL sample [31].

3.6. Wettability Analysis

The contact angle was measured with the Ramé-Hart NRL A 100-00 goniometer to evaluate the wettability of the electrospun films. Distilled water (2 μL) was deposited on the surface of a 1 cm x 4 cm sample at room temperature.

3.7. Water Vapour Transpiration Rate Analysis

Furthermore, a water vapour permeation test was performed on electrospun samples for seven days following ASTM D 1653. A permeability cup (Payne cup) filled with 10 g of distilled water and the electrospun film sample fixed on its opening was placed inside a closed glass chamber at room temperature, along with a sodium pentoxide ($C_5H_{11}NaO$) reservoir. Evaporation through the films was monitored by measuring the weight loss of the cup at initial intervals of 15 minutes until the second hour, then at intervals of 1 hour until the seventh hour, and then, finally, at intervals of 24 hours until the end of 7 days. Weight loss was calculated using Equation 2.

$$J = \frac{\Delta m}{\Delta t} * A \quad (2)$$

Where J is water vapour flux, Δm is the mass difference, Δt is the time difference and A is film area [73].

3.8. Propolis Release Assay

A propolis release test on PCL + propolis samples was also carried out in saline solu, at 37 ºC, 100 rpm, for up to 2 days (N=3). Samples of 1 cm x 1 cm were placed in 2 mL saline solution and collected at the following times: 0.5, 2, 24, and 48 hours. The amount of propolis released was quantified on the UV-Vis Perkin Elmer Lambda 25 spectrophotometer at 302 nm.

Preprints (www.preprints.org) | NOT PEER-REVIEWED | Posted: 1 July 2022 doi:10.20944/preprints202207.0023.v1

3.9. Scratch Wound Assay

Human gingival fibroblast (FGH) cell lines (2×10^5 cells) were seeded in 24-well plates and allowed to attach for 24 h at 37ºC. Simulated wounds were created in confluent cells using a pipette tip. Cells were then rinsed with a medium to remove floating cells and debris. After washing, cells were cultivated in the presence of electrospun PCL/Prop films for another 24 h. The culture plates were incubated at 37 °C. Cells cultivated without any film were used as control. Wound gaps were measured at 0 and 24 h, using an inverted microscope equipped with a digital camera. The percentage of wound-healing was determined as the difference between the gap lengths according to the Equation 3 [74].

$$\%\, Wound\ closure\ = Average\ of \left(\frac{[Gap\ length]_{0h} - [Gap\ length]_{24h}}{[Gap\ length]_{0h}} \right) \quad (3)$$

4. Conclusion

In this work, it was possible to produce electrospun films composed of fibres, beaded fibres, and beads using 30 wt.% PCL, with and without 15 % (v/v) alcoholic propolis extract. A more eco-friendly solvent system composed of acetic acid/formic acid was employed, With the natural extract acting as a lubricating agent, as seen in viscosity analyses, the films morphology variation ca be attributed to the hydrolysis of the ester bonds of PCL that decreased its molecular weight by approximately half every seven days of storage time. The PCL hydrolysis also influenced the structural arrangements of the polymer spherulites, thus allowing an increase in the material crystallinity regardless of the presence of propolis, especially in films with beads structures. All films were in an ideal range of water vapour transpiration rate, with rates in the spectrum of commercial products. The incorporation of propolis alcoholic extract significantly increases the hydrophilicity of the films if compared to pure PCL structures, which could promote better environment to support cellular event during wound healing process. Furthermore, even though the bead structures addition in films did not alter the burst release pattern, the presence of beads combined with fibres in PCL/Prop beaded fibre film had the better result in the wound healing assay with human gingival fibroblast (FGH) cells, with a trend towards accelerating healing in 24 hours. These films presented the potential for wound dressing application, encouraging further biological experiments.

Author Contributions: **A. C. de Figueiredo:** Methodology, Investigation, Visualisation, Formal analysis, Writing - Review & Editing, Writing - Original Draft Preparation; **J. M. A. Mancipe:** Methodology, Project administration, Investigation, Visualisation, Formal analysis, Writing - Review & Editing, Writing - Original Draft Preparation; **A. O. da Silva de Barros:** Investigation, Writing - Original Draft Preparation; **R. Santos-Oliveira:** Investigation, Writing - Original Draft Preparation, Funding acquisition; **M. L. Dias:** Resources, Writing - Review & Editing; **R. M. S. M. Thiré:** Conceptualization, Methodology, Supervision, Project administration, Resources, Funding acquisition, Writing - Review & Editing. All authors have read and agreed to the published version of the manuscript.

Funding: The authors are grateful to the following Brazilian agencies: CAPES, CNPq (Grants 308789/2020-2, and 308789/2020-2), and FAPERJ (Grants: Temáticos - E-26/211.269/2021, and Rede NanoSaúde - E-26/210.139/2019) for financial support.

Acknowledgments: We would like to express our gratitude to the Multi-user Nucleus of Microscopy of the Metallurgical and Materials Engineering Program (PEMM)/COPPE/UFRJ for SEM analysis, to the Thermal Analysis and Rheology Laboratory, allocated in the Center for Biofuels, Petroleum and its Derivatives (EQ/UFRJ) for the rheological experiments assistance and to the Surface Modification and Characterisation Laboratory – LabAFM of PEMM/UFRJ for the contact angle measurements.

 doi:10.20944/preprints202207.0023.v1

Conflicts of Interest: The authors declare no conflict of interest. The funders had no role in the design of the study; in the collection, analyses, or interpretation of data; in the writing of the manuscript; or in the decision to publish the results.

References

[1]. M.E. El-Naggar, E.S. Shalaby, A.H. Abd-Al-Aleem, M.A. Abu-Saied, A.M. Youssef. Synthesis of environmentally benign antimicrobial dressing nanofibres based on polycaprolactone blended with gold nanoparticles and spearmint oil nanoemulsion. Journal of Materials Research and Technology (2021), 15:3447-3460. https://doi.org/10.1016/j.jmrt.2021.09.136

[2]. R.S. Ambekar, B. Kandasubramanian. Advancements in nanofibres for wound dressing: A review", European Polymer Journal (2019); 117:304-336. https://doi.org/10.1016/j.eurpolymj.2019.05.020

[3]. J.M.A. Mancipe, F.A. Lobianco, M.L. Dias, R.M.S.M. Thiré. Electrospinning: New strategies for the treatment of skin melanoma, Mini-Reviews in Medicinal Chemistry (2022); 22(4):564-578. https://doi.org/10.2174/1389557521666210712111809

[4]. A. Haider, S. Haider, IK. Kang. A comprehensive review summarizing the effect of electrospinning parameters and potential applications of nanofibres in biomedical and biotechnology. Arabian Journal of Chemistry (2018); 11(8):1165-1188. https://doi.org/10.1016/j.arabjc.2015.11.015

[5]. C.R. Lynch, P.P Kondiah, Y. E. Choonara. Advanced strategies for tissue engineering in regenerative medicine: A biofabrication and biopolymer perspective. Molecules (2021); 26(9): 2518. https://doi.org/10.3390/molecules26092518

[6]. C. Wang, J. Wang, L. Zeng, Z. Qiao, X. Liu, H. Liu, J. Zhang, J. Ding. Fabrication of electrospun polymer nanofibers with diverse morphologies. Molecules (2019); 24(5): 834. https://doi.org/10.3390/molecules24050834

[7]. M.E. El-Naggar, O.A.A. Abu, D.I. Saleh, M.A. Abu-Saied, M.K. Ahmed, E. Abdel-Fattah, et al. Facile modification of polycaprolactone nanofibres with hydroxyapatite doped with thallium ions for wound and mucosal healing applications. Journal of Materials Research and Technology (2021); 15:2909-2917. https://doi.org/10.1016/j.jmrt.2021.09.057

 doi:10.20944/preprints202207.0023.v1

[8]. V.R. Viana, W.H. Ferreira, E.G. Azero, M.L. Dias, C.T. Andrade. Optimization of electrospinning conditions by Box-Behnken design to prepare poly(vinyl alcohol)/chitosan crosslinked nanofibres. Journal of Materials Science and Chemical Engineering (2020); 8(4):13-31. https://doi.org/ 10.4236/msce.2020.84002

[9]. S. Kajdič, O. Planinšek, M. Gašperlin, P. Kocbek. Electrospun nanofibres for customized drug–delivery systems. Journal of Drug Delivery Science and Technology (2019); 51:672-681. https://10.1016/j.jddst.2019.03.038

[10]. H. Zhao, H. Chi. Electrospun bead-on-string fibres: useless or something of value. In: Tong Lin. Editors, Novel aspects of nanofibres, IntechOpen, London, 2018, pp. 87-102. Doi: 10.5772/intechopen.74661

[11]. T. Li, X. Ding, L. Tian, J. Hu, X. Yang, S. Ramakrishna. The control of beads diameter of bead-on-string electrospun nanofibres and the corresponding release behaviors of embedded drugs. Materials Science and Engineering: C (2017); 74:471-477. https://doi.org/10.1016/j.msec.2016.12.050

[12]. R.T. Steipel, M.D. Gallovic, C.J. Batty, E.M. Bachelder, K.M. Ainslie. Electrospray for generation of drug delivery and vaccine particle applied in vitro and in vivo. Materials Science and Engineering: C (2019); 105:110070. https://10.1016/j.msec.2019.110070

[13]. B. Joseph, R. Augustine, N. Kalarikkal, S. Thomas, B. Seantier, Y. Grohens. Recent advances in electrospun polycaprolactone based scaffolds for wound healing and skin bioengineering applications. Materials Today Communications (2019); 19:319-335. https://doi.org/10.1016/j.mtcomm.2019.02.009

[14]. D. Mondal, G. May, S.S. Venkatraman. Polycaprolactone-based biomaterials for tissue engineering and drug delivery: Current scenario and challenges. International Journal of Polymeric Materials and Polymeric Biomaterials (2016); 65(5):255-265. https://doi.org/10.1080/00914037.2015.1103241

[15]. Ž. Peršurić, S. K. Pavelić. Bioactives from Bee Products and Accompanying Extracellular Vesicles as Novel Bioactive Components for Wound Healing. Molecules (2021); *26*(12), 3770.

https://doi.org/10.3390/molecules26123770

[16]. C. Stefano, F. Capasso. Propolis, an old remedy used in modern medicine. Fitoterapia (2002); 73:S1-S6. https://doi.org/10.1016/S0367-326X(02)00185-5

[17]. R.N. Oliveira, G.B. McGuinness, M.E.T. Ramos, C.E. Kajiyama, R.M.S.M. Thiré. Properties of PVA Hydrogel Wound-Care Dressings Containing UK Propolis. Macromolecular Symposia (2016); 368(1):122-127. https://doi.or/10.1002/masy.201500149

[18]. R.N. Oliveira, A.P.D. Moreira, R.M.S.M. Thiré, B. Quilty, T.M. Passos, P. Simon, et al. Absorbent polyvinyl alcohol-sodium carboxymethyl cellulose hydrogels for propolis delivery in wound healing applications. Polymer Engineering and Science (2017); 57(11):1224-1233. https://doi.org/10.1002/pen.24500

[19]. Z. Li, J. Li, G. Wang, Y. Tao, X. Chang, H. Xia, et al. Reviewing Propolis with Multi-components in the Treatment of Oral Diseases through Multi-pathways and multi-targets. Mini-Reviews in Medicinal Chemistry (2021); 21(12):1406-1420. https://doi.org/10.2174/1389557521666210126141314

[20]. R.N. Oliveira, G.B. McGuinness, R. Rouze, B. Quilty, P. Cahill, G.D.A. Soares, et al. PVA hydrogels loaded with a Brazilian propolis for burn wound healing applications. Journal Applied Polymer Science (2015); 132(25):42129. https://doi.org/10.1002/app.42129

[21]. M. Stojko, J. Wlodarczyk, M. Sobota, P. Karpeta-Jarzabek, M. Pastusiak, H. Janeczek, et al. Biodegradable Electrospun Nonwovens Releasing Propolis as a Promising Dressing Material for Burn Wound Treatment, Pharmaceutical (2020); 12(9):883. https://doi.org/10.3390/pharmaceutics12090883

[22]. T.B. Alberti, D.S. Coelho, M. de Prá, M. Maraschin, M. Maraschin, et al. Electrospun PVA nanoscaffolds associated with propolis nanoparticles with wound healing activity, Journal of Materials Science (2020); 55(23):9712-9727. https://doi.org/10.1007/s10853-020-04502-z

[23]. G. Salimbeigi, R.N. Oliveira, G.B. McGuinness. Electrospun poly(ε-caprolactone)/propolis fibre morphology: A process optimization study. Journal of Applied Polymer Science (2022); 139(19):52131. https://doi.org/10.1002/app.52131

[24]. M. Atari, Z. Mohammadalizadeh, A.Z. Kharazi, S.H. Javanmard. The effect of different solvent systems on physical properties of electrospun poly(glycerol sebacate)/poly(ε-caprolactone) blend, Polymer-Plastics Technology and Materials (2022). 61(7):789-802. https://doi.org/10.1080/25740881.2021.2022161

[25]. Y. Mao, M. Chen, R. Guidoin, Y. Li, F. Wang, G. Brochu, et al. Potential of a facile sandwiched electrospun scaffolds loaded with ibuprofen as an anti-adhesion barrier. Materials Science and Engineering: C (2021); 118:111451. https://doi.org/10.1016/j.msec.2020.111451

[26]. M. Shahrousvand, V. Haddadi-Asl, M. Shahrousvand. Step-by-step design of poly((ε-caprolactone)/chitosan/melilotus Officinalis extract electrospun nanofibres for wound dressing applications, International Journal of Biological Macromolecules (2021); 180:36-50. https://doi.org/10.1016/j.ijbiomac.2021.03.046

[27]. J.M.A. Mancipe, M.L. Dias, R.M.S.M. Thiré. Morphological evaluation of electrospun polycaprolactone fibres depending on the type of solvent. Revista Matéria (2019); 24(3):e-12400. https://doi.org/10.1590/S1517-707620190003.0713

[28]. L. Van der Schueren, B. De Schoenmaker, Ö.I. Kalaoglu, K. De Clerck. An alternative solvent system for the steady state electrospinning of polycaprolactone. European Polymer Journal (2011); 47(6):1256-1263. https://doi.org/10.1016/j.eurpolymj.2011.02.025

[29]. L. Malinová, M. Stolínová, D. Lubasová, L. Martinová, J. Brožek. Electrospinning of polyesteramides based on ε-caprolactam and ε-caprolactone from solution. European Polymer Journal (2017); 49(10):3135-3143. https://doi.org/10.1016/j.eurpolymj.2013.07.015

 doi:10.20944/preprints202207.0023.v1

[30]. N. Lavielle, A.M. Popa, M. de Geus, A. Hébraud, G. Schalatter, L. Thöny-Meyer, et al. Controlled formation of poly (ε-caprolactone) ultrathin electrospun nanofibres in a hydrolytic degradation-assisted process. European Polymer Journal (2013); 49(6):1331-1336. https://doi.org/10.1016/j.eurpolymj.2013.02.038

[31]. J. Dulnik, P. Dennis, P. Sajkiewicz, D. Kolbuk, E. Choinska. Biodegradation of bicomponent PCL/gelatin and PCL/collagen nanofibres electrospun from alternative solvent system. Polymer Degradation and Stability (2016); 130:10-21. https://doi.org/10.1016/j.polymdegradstab.2016.05.022

[32]. O. Gil-Castell, J.D. Badia, E. Strömberg, S. Karlsson, A. Ribes-Greus. Effect of the dissolution time into an acid hydrolytic solvent to tailor electrospun nanofibrous polycaprolactone scaffolds. European Polymer Journal (2017); 87:74-187. https://doi.org/10.1016/j.eurpolymj.2016.12.005

[33]. C. Ramos, G.M. Lanno, I. Laidmäe, A. Meos, R. Harmas, K. Kogermann. High humidity electrospinning of porous fibres for tuning the release of drug delivery systems. International Journal of Polymeric Materials and Polymeric Biomaterials (2020): 1-13. https://doi.org/10.1080/00914037.2020.1765361

[34]. M.A. Elnaggar, H.A. El-Fawal, N.K. Allam. Biocompatible PCL-nanofibres scaffold with immobilized fibronectin and laminin for neuronal tissue regeneration. Materials Science and Engineering: C (2021); 119:111550. https://doi.org/10.1016/j.msec.2020.111550

[35]. S. Homaeigohar, M. Monavari, B. Koenen, A.R. Boccaccini. Biomimetic biohybrid nanofibres containing bovine serum albumin as a bioactive moiety for wound dressing. Materials Science and Engineering: C (2021); 123:111965. https://doi.org/10.1016/j.msec.2021.111965

[36]. R. N. Oliveira, A. P. D. Moreira, R. M. S. M. Thiré, B. Quilty, T.M. Passos, P. Simon, M.C. Mancini, G. B. McGuinness. Absorbent polyvinyl alcohol–sodium carboxymethyl cellulose hydrogels for propolis delivery in wound healing applications. Polymer Engineering & Science (2017); 57(11): 1224-1233. https://doi.org/10.1002/pen.24500

 doi:10.20944/preprints202207.0023.v1

[37]. N. Ibrahim, A. J. Zakaria, Z. Ismail, Y. Ahmad, K. S. Mohd. Application of GCMS and FTIR fingerprinting in discriminating two species of Malaysian stingless bees propolis. International Journal of Engineering and Technology (2018); 7: 106-112. https://doi.org/10.14419/ijet.v7i4.43.25828

[38]. R. N. Oliveira, M. C. Mancini, F.C.S.D. Oliveira, T.M. Passos, B. Quilty, R.M.S.M. Thiré, G. B. McGuinness. FTIR analysis and quantification of phenols and flavonoids of five commercially available plants extracts used in wound healing. Matéria (Rio de Janeiro)(2016); 21: 767-779. https://doi.org/10.1590/S1517-707620160003.0072

[39]. L. Svečnjak, Z. Marijanović, P. Okińczyc, P. Marek Kuś, I. Jerković. Mediterranean propolis from the Adriatic Sea islands as a source of natural antioxidants: comprehensive chemical biodiversity determined by GC-MS, FTIR-ATR, UHPLC-DAD-QqTOF-MS, DPPH and FRAP assay. Antioxidants (2020); *9*(4), 337. https://doi.org/10.3390/antiox9040337

[40]. A.B. Moghaddam, B. Shirvani, M.A. Aroon, T. Nazari. Physico-chemical properties of hybrid electrospun nanofibres containing polyvinylpyrrolidone (PVP), propolis and aloe vera. Materials Research Express (2018); 5:125404. https://org.org/10.1088/2053-1591/aae0bf

[41]. SV. Canevarolo-Junior. Ciência dos Polímeros: Um texto Básico para Tecnólogos e Engenheiros, 2nd ed, Artliber: São Paulo; 2006.

[42]. J. Dias, F. Antunes, P. Bartolo. Influence of the rheological behavior in electrospun PCL nanofibres production for tissue engineering applications. Chemical Engineering Transactions (2013); 32:1015-1020. https://doi.org/10.3303/CET1332170

[43]. E.B. Gurler, N.M. Ergul, B. Ozbek, N. Ekren, F.N. Oktar, M.E. Haskoylu, et al. Encapsulated melatonin in polycaprolactone (PCL) microparticles as a promising graft material. Materials Science and Engineering: C (2019); 100:798-808. https://doi.org/10.1016/j.msec.2019.03.051

[44]. M. Zhang, T. Kiratiwongwan, W. Shen. Oxygen-releasing polycaprolactone /calcium peroxide composite microspheres. Journal of Biomedical Materials Research Part B: Applied Biomaterials (2020); 108(3):1097-1106. https://doi.org/10.1002/jbm.b.34461

[45]. A.I.S. Morais, E.G. Vieira, S. Afewerki, R.B. Sousa, L.M. Honorio, A.N.C.O. Cambrussi, et al. Fabrication of polymeric microparticles by electrospray: the impact of experimental parameters. Journal of functional biomaterials (2020); 11:4. https://doi.org/10.3390/jfb11010004

[46]. K. Sutjarittangtham, T. Tunkasiri, P. Chantawannakul, U. Intatha, S. Eitssayeam. Mechanical improved antibacterial polycaprolactone/propolis electrospun fiber mat by adding bacterial nanocellulose, Journal of Computational and Theoretical Nanoscience (2015); 12:798-803. https://doi.org/10.1166/jctn.2015.3806

[47]. M.C.G. Pedrosa, S.A. dos Anjos, E. Mavropoulos, P.L. Bernardo, J.M. Granjeiro, A.M. Rossi, et al. Structure and biological compatibility of polycaprolactone/zinc-hydroxyapatite electrospun nanofibers for tissue regeneration, Journal of Bioactive and Compatible Polymers (2021); June. https://doi.org/10.1177/08839115211022448

[48]. M.J. Jenkins, K.L. Harrison. The effect of molecular weight on the crystallization kinetics of polycaprolactone. Polymers advanced Technology (2006); 17(4):474-478. https://doi.org/10.1002/pat.733

[49]. S. Mahalakshmi, T. Alagesan, V. Parthasarathy, K.L. Tung, R. Anbarasan. Non-isothermal crystallization kinetics and degradation kinetics studies on barium thioglycolate end-capped poly(ε-caprolactone). Journal of Thermal Analysis and Calorimetry (2019); 135:3129-3140. https://doi.org/10.1007/s10973-018-7514-2

[50]. MS. Karizmeh, S.A. Poursamar, A. Kefayat, Z. Farahbakhsh, M. Rafienia. An *in vitro* and *in vivo* study of PCL/chitosan electrospun mat on polyurethane/propolis foam as a bilayer wound dressing. Materials Science and Engineering: C (2022); 112667. https://doi.org/10.1016/j.msec.2022.112667

[51]. A.L.M.M. Toledo, B.S. Ramalho, P.H.S. Picciani, L.S. Baptista, A.M.B. Martinez, M.L. Dias. Effect of three different amines on the surface properties of electrospun polycaprolactone mats. International Journal of Polymeric Material and Polymeric Biomaterials (2020); 1–13. https://doi.org/10.1080/00914037.2020.1785463

[52]. M.C. Marcucci. Propolis: chemical composition, biological properties and therapeutic activity. Apidologie (1995); 26(2):83-99.

https://doi.org/10.1051/apido:19950202

[53]. M. Franchin, I.A. Freire, J.G. Lazzarini, B.D. Nani, M.G. da Cunha, D.F. Colón, et al. The use of Brazilian propolis for discovery and development of novel anti-inflammatory drugs. European Journal of Medicinal Chemistry (2018); 153:49-55. https://doi.org/10.1016/j.ejmech.2017.06.050

[54]. L. Li, Y. Wang, K. Liu, L. Yang, B. Zhang, Q. Luo, et al. Nanoparticles-stacked superhydrophilic coating supported synergistic antimicrobial ability for enhanced wound healing. Materials Science and Engineering: C (2022); 132:112535. https://doi.org/10.1016/j.msec.2021.112535

[55]. W. Jia, J.A. Kharraz, P.J. Choi, J. Guo, B.J. Deka, A.K. An. Superhydrophobic membrane by hierarchically structured PDMS-POSS electrospray coating with cauliflower-shaped beads for enhanced MD performance. Journal of Membrane Science (2020); 597:117638. https://doi.org/10.1016/j.memsci.2019.117638

[56]. J.M. de Oliveira, L.H.I. Mei. Nonionic reactive surfactants in emulsion polymerization of vinyl acetate - vinyl neodecanoate latexes: Influence on the water barrier properties. Polímeros (2009): 19:23-30. https://doi.org/10.1590/S0104-14282009000100009

[57]. K. Nuutila, E. Eriksson. Moist wound healing with commonly available dressing. Advances in wound care (2021); 10(12):685-698. https://doi.org/10.1089/wound.2020.1232

[58]. Y.B. Wu, S.H. Yu, F.L. Mi, C.W. Wu, S.S. Shyu, C.K. Peng, et al. Preparation and characterization on mechanical and antibacterial properties of chitosan/cellulose blends. Carbohydrate Polymers (2004); 57(4):435-440. https://doi.org/10.1016/j.carbpol.2004.05.013

[59]. X. Zhang, L. Yang, C. Zhang, D. Liu, S. Meng, W. Zhang, et al. Effect to polymer Permeability and Solvent Removal Rate on In Situ Forming Implants: Drug Burst Release and Microstructure. Pharmaceutics (2019); 11(10):520. https://doi.org/10.3390/pharmaceutics11100520

 doi:10.20944/preprints202207.0023.v1

[60]. R. Ramalingam, C. Dhand, C.M. Leung, H. Ezhilarasu, P. Prasannan, S.T. Ong, et al. Poly-ε-Caprolactone/Gelatina hybrid Electrospun Composite Nanofibrous Mats Containing Ultrasound Assisted Herbal Extract: Antimicrobial and Cell Proliferation study, Nanomaterials (2019); 9(3):462. https://doi.org/10.3390/nano9030462

[61]. T. Maver, M. Kurečič, T. Pivec, U. Maver, L. Gradišnik, P. Gašparič, et al. Needleless electrospun carboxymethyl cellulose/polyethylene oxide mats with medicinal plant extracts for advanced wound care applications. Cellulose (2020); 27:4487-4508. https://doi.org/10.1007/s10570-020-03079-9

[62]. Š. Zupančič, L. Preem, J. Kristl, M. Putrinš, T. Tenaon, P. Kocbek, et al. Impact of PCL nanofibre mat structural properties on hydrophilic drug release and antibacterial activity on periodontal pathogens. European Journal of Pharmaceutical Science (2018); 122:347-358. https://doi.org/10.1016/j.ejps.2018.07.024

[63]. C.R. Reshmi, P.S. Suja, O. Manaf, P.P. Sanu, A. Sujith. Nanochitosan enriched poly ε-caprolactone electrospun wound dressing membranes: A fine tuning of physicochemical properties, hemocompatibility and curcumin release profile. International journal of biological macromolecules (2018); 108:1261-1272. https://doi.org/10.1016/j.ijbiomac.2017.11.035

[64]. A. Jacob, A. Parolia, A. Pau, F.D. Amalraj. The effects of Malaysian propolis and Brazilian red propolis on connective tissue fibroblasts in the wound healing process. BMC Complementary and Alternative Medicine (2015); 15:294. https://doi.org/10.1186/s12906-015-0814-1

[65]. E. Rojczyk, A. Klama-Baryla, W. Łabuś, K. Wilemska-Kucharzewska, M. Kucharzewski. Historical and modern research on propolis and its application in wound healing and other fields of medicine and contributions by Polish studies. Journal of Ethnopharmacology (2020); 262:113159. https://doi.org/10.1016/j.jep.2020.113159

[66]. M. Behyari, R. Imani, H. Keshvari. Evaluation of skin fibroin nanofibrous dressing incorporation niosomal propolis, for potential use in wound healing. fibres and Polymers (2021); 22:2090-2101. https://doi.org/10.1007/s12221-021-0973-2

[67]. A. Oryan, E. Alemzadeh, A. Moshiri. Potential role of propolis in wound healing: Biological properties and therapeutic activities. Biomedicine & Pharmacotherapy (2018); 98:469-483. https://doi.org/10.1016/j.biopha.2017.12.069

[68]. P. Ebadi, M. Fazeli. Evaluation of the potential in vitro effects of propolis and honey on wound healing in human dermal fibroblast cells. South African Journal of Botany (2021); 137:414-422. https://doi.org/10.1016/j.sajb.2020.10.003

[69]. H.C. Rosseto, L.A.S. de Toledo, L.M.B. de Francisco, E. Esposito, Y. Lim, G. Valacchi, et al. Nanostructured lipid systems modified with waste material of propolis for wound healing: Design, in vitro and in vivo evaluation. Colloids and Surfaces B: Biointerfaces (2017); 158:441-452. https://doi.org/10.1016/j.colsurfb.2017.07.029

[70]. R. Tayfeh-Ebrahimi, A. Amniattalab, R. Mohammadi. Evaluation of Effect of Biologically Synthesized Ethanolic Extract of Propolis-Loaded Poly (-Lactic-co-Glycolic Acid) Nanoparticles on Wound Healing in Diabetic Rats. The International Journal of Lower Extremity Wounds (2022); January:2022. https://doi.org/10.1177/15347346211073224

[71]. T.B. Alberti, D.S. Coelho, M. de Prá, M. Maraschin, B. Veleirinho. Electrospun PVA nanoscaffolds associated with propolis nanoparticles with wound healing activity. Journal of Materials Science (2020); 55:9712-9727. https://doi.org/10.1007/s10853-020-04502-z

[72]. I. Bonadies, F. Cimino, V. Guarino. In vitro degradation of zein nanofibres for propolis release in oral treatments. Materials Research Express (2019); 6:075407. https://doi.org/10.1088/2053-1591/ab178e

[73]. G. Rodrigues-Filho, D.S. Monteiro, C.S. Meireles, R.M.N. De Assunção, D.A. Cerqueira, H.S. Barud, et al. Synthesis and characterization of cellulose acetate produced from recycled newspaper, Carbohydrate Polymers (2008); 73:74-82. https://doi.org/10.1016/j.carbpol.2007.11.010

[74]. S. Martinotti, E. Ranzato. Scratch Wound Healing Assay. In: Turksen K. (eds) Epidermal Cells. Methods in Molecular Biology, vol 2109. Humana, New York, NY. (2019), p. 225-229. https://doi.org/10.1007/7651_2019_259